Applied Water Science (2022) 12:71
https://doi.org/10.1007/s13201-022-01585-8

ORIGINAL ARTICLE

GIS-based multi-criteria approach to delineate groundwater prospect zone and its sensitivity analysis

Mukesh Kumar[1] · Sudhir Kumar Singh[2] · Arnab Kundu[3] · Krishan Tyagi[4] · Jagadeesh Menon[4] · Alex Frederick[1] · Aditya Raj[5] · Deepak Lal[1]

Received: 21 July 2021 / Accepted: 3 February 2022 / Published online: 21 March 2022

Abstract

This study was aimed at delineating groundwater potential zones (GWPZ) using geo-spatial techniques for Ranchi district, Jharkhand (India). Data including Cartosat-1 digital elevation model (DEM), Landsat 8 satellite images, lithology, geology, soil, and water yield data were utilised in this study. The relative importance of multiple parameters including lithology, soil, slope, geology, rainfall, drainage density, and land use/land cover (LULC) that influence the availability of groundwater was determined subjectively. Analytical hierarchy process (AHP) along with pair-wise comparison decision theory was utilized to calculate the weights for each aforementioned parameter. The delineated GWPZ were categorized into four classes viz., very good zone (31.57%), good zone (45.43%), moderate zone (13.09%), and poor zone (8.53%). The sensitivity analysis indicated lithology and soil type as the most and least sensitive parameters, respectively influencing the presence of groundwater in the study area. Comparison between well discharge data and delineated GWPZ yielded a coefficient of determination (R^2) of 0.59. This study contributes to identifying priority areas where appropriate water conservation programs as well as strategies for sustainable groundwater development can be implemented.

Keywords Pair-wise comparison · Decision making · Groundwater instability · Multi-influencing factors · Ranchi (India)

Introduction

Groundwater serves as an important resource of fresh water for domestic, agricultural, animal husbandry, industrial activities, and other multipurpose uses (Singh et al. 2009). The over-utilization of groundwater resources without implementing proper management/recharge policies causes depletion in the groundwater table. The planning and management of groundwater resources gets complicated under changing climate.

Exploring new sites of groundwater rely on the integration of geophysical, aeromagnetic surveys along with the remote sensing (RS) and the geographical information system (GIS) (Mukherjee et al. 2007). Remote sensing and GIS

✉ Sudhir Kumar Singh
sudhirinjnu@gmail.com

Mukesh Kumar
mukeshkumar.fo@gmail.com

Arnab Kundu
arnknd@gmail.com

Krishan Tyagi
krishantyagi75@gmail.com

Jagadeesh Menon
jagadeeshmenon.m@gmail.com

Alex Frederick
alex.frederick65@gmail.com

Aditya Raj
raj05aditya@gmail.com

Deepak Lal
deepakl@shiats.edu.in

[1] Centre for Geospatial Technologies, Sam Higginbottom University of Agriculture, Technology and Sciences, Prayagraj, Uttar Pradesh 211007, India

[2] K. Banerjee Centre of Atmospheric and Ocean Studies, Nehru Science Centre, IIDS, University of Allahabad, Prayagraj, Uttar Pradesh 211002, India

[3] Department of Geo-Informatics, P.R.M.S. Mahavidyalaya, Bankura University, Bankura, West Bengal 722150, India

[4] Deutsche Gesellschaft Für Internationale Zusammenarbeit (GIZ), New Delhi, India

[5] School of Computer and Systems Sciences, Jawaharlal Nehru University, New Delhi 10067, India

techniques have been found to be effective and gained popularity in delineating the GWPZ (Singh et al. 2010; Duran-Llacer et al. 2022). Researchers have used various RS and GIS-based techniques to delineate GWPZ including fuzzy sets (Bellman and Zadeh 1970; Aouragh et al. 2017), Multi-Criteria Decision Making and Dempster-Shafer Model (Pandey et al. 2022), linguistic variables (Chen and Hwang 1992), multi-influencing factors (Anbarasu et al. 2020; Pande et al. 2021; Sikakwe 2020), multi-criteria decision-making and Boolean logic modeling (Machiwal and Singh 2015), MCDM–AHP (Kumar and Pandey 2016; Agarwal and Garg 2016; Nag and Kundu 2018), decision tree (Duan et al. 2016), weights of evidence (Pourtaghi and Pourghasemi 2014), random forest (Chen et al. 2019), frequency ratio (Trabelsi et al. 2019), weight of evidence and artificial neural network (Corsini et al. 2009; Lee et al. 2018; Lee et al. 2020), logistic regression (Park et al. 2017), and entropy (Al-Abadi et al. 2016; Rahmati et al. 2016) models. Analytical hierarchy process (AHP) is among the most popular and frequently used method for determining GWPZ (Murmu et al. 2019: Das 2019; Kumari and Singh 2021).

The present study utilized and investigated the integrated application of remote sensing, GIS, and AHP techniques for delineating GWPZ in the Ranchi district, Jharkhand (India).

Study area

The district of Ranchi has a municipal area of 652.02 km^2 with an average elevation of 651 m above sea level and is located between 23°22′N latitude and 85°20′E longitude (Fig. 1). Ranchi is the capital of Jharkhand state. The entire district is located in the eastern section of the Deccan plateau, particularly in the southern part of the Chota Nagpur plateau, surrounded by lush agriculturally fertile land (CGWB 2013). Due to the presence of hilly topography and dense tropical forests, Ranchi experiences a relatively moderate climate as compared to the rest of the state.

According to Köppen Climate Classification, Ranchi experiences a humid subtropical climate (Cwa). The temperature of Ranchi ranges between 0 to 25 °C in winters, while in summers, it ranges between 20 to 42 °C. The rainfall in Ranchi between June and September is 1100 mm, while the annual rainfall is 1430 mm.

Damodar, Subarnarekha, South Koel, and Karari are the important river basins of the study area. The eastern part of the study area is drained by River Subarnarekha with its tributaries Kanchi and Raru while River South Koel and Karo drains the western part. The southeastern part of the district is drained by River Karkari. Ranchi has a total area of 5, 09,700 hectares out of which, net sown area, forests, fallow, land other than current fallow, land put to non-agricultural use and barren land are 33.64%, 20.97%, 16.35%, 8.7%, 5.6%, and 4.2%, respectively. The area is sown more than once and cultivable wastelands are 2.21% and 3.4%, respectively.

Material and methods

Data used

Cartosat-1 DEM data was used to generate a slope map. It was downloaded from the Bhuvan portal of the National Remote Sensing Centre (NRSC) /Indian Space Research Organisation (ISRO) (www.bhuvan.nrsc.gov.in). DEM data was utilized to extract information about the slope, elevation, drainage pattern, etc. of the study area. Landsat 8 satellite data was used to derive information about lineaments and land use/land cover in the present study. The satellite data utilized in the present study were downloaded from the Earth Explorer, United States Geological Survey (USGS) site (www.earthexplorer.usgs.gov). Tropical Rainfall Measurement Mission (TRMM) datasets (3B43) were used to generate a rainfall map for the study area.

Well discharge data of the study area with their location points were obtained from the Central Ground Water Board (CGWB). Well discharge data were used to compare the delineated GWPZ.

Generation of thematic layers

Total eight thematic layers, namely geomorphology, lithology, land use/land cover, drainage density, rainfall, soil, slope, and lineament density, were prepared to assess groundwater potential zone with the aid of remote sensing and GIS techniques.

Figure 2 illustrates an overview of the adopted methodology.

Lithology

Lithology describes the physical characteristics of rock, including colour, composition, and texture. It is an important factor in detecting GWPZ as it influences the permeability and the porosity of aquifer rocks (Rahmati et al. 2015). The lithology map for the study area was obtained from the Geological Survey of India (GSI) and digitized in a GIS environment.

Geomorphology

Geomorphology is a relevant factor in the evaluation of GWPZ as it influences the subsurface movement of groundwater. Geomorphology for the study area was obtained from Landsat 8 satellite data by utilizing its three spectral bands (green, red and near-infrared). Haze reduction technique was

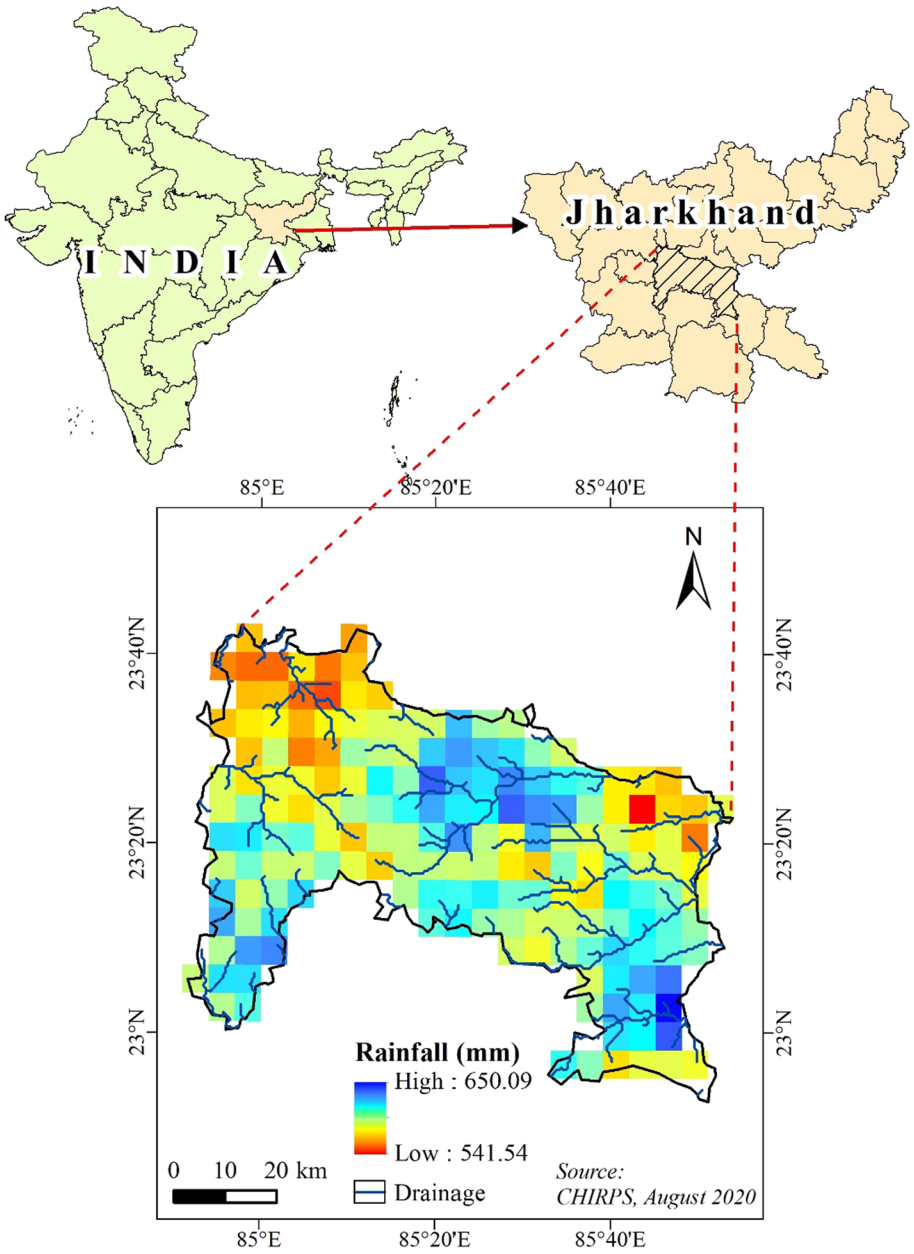

Fig. 1 Location map of the study area

followed to improve the interpretability and quality of satellite data. Finally, the geomorphology map was generated by digitizing (in a GIS environment) different geomorphological features that were apparent in the study area.

Slope

Slope is a major factor that controls the infiltration of surface water into the sub-surface, indicating the suitability for groundwater recharge (Kumar et al. 2018). An area with a high slope has high runoff with less residence time for water while a gentle slope, facilitate more time for percolation of water with slow surface runoff (Prasad et al. 2008; Magesh et al. 2012). Slope map of the study area was prepared using Cartosat-1 DEM data.

Soil

Groundwater recharge is dependent on the rate of infiltration, percolation, permeability, and type of soil (Patle et al. 2019; Singh et al. 2020). Soil texture plays an important role in groundwater recharge and runoff.

The soil map of the study area was downloaded in vector format at a scale of 1:50,000 from the soil map of the world website (https://worldmap.harvard.edu). The study area was found to be mostly characterized by residual type

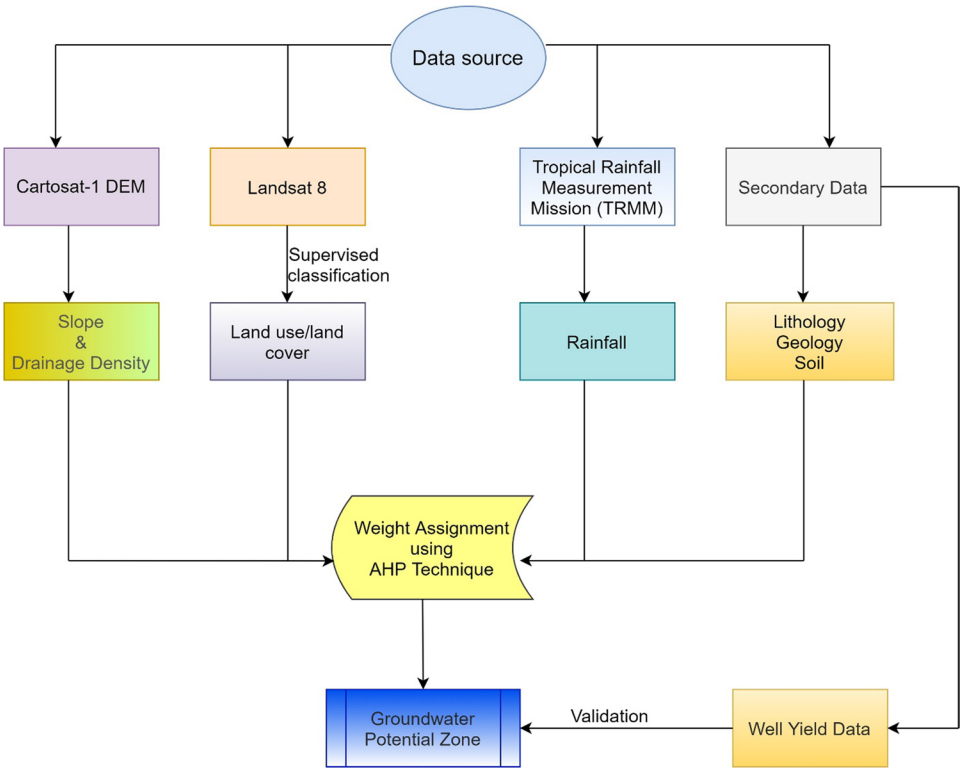

Fig. 2 Flow chart of methodology

of soil. Patches of Lateritic type of soil also appeared in the greater part of the district, particularly in rocks of Archean metamorphic complex. Based on textural characteristics, the soil of the study area could be classified into three major classes: (i) Red and yellow soil-These soils are formed due to the decomposition of crystalline metamorphic rocks like granite-gneiss, etc., also containing mineral particles like hornblende, iron, and biotite. The low-lying areas carry comparatively a dark red color in comparison to higher areas which have a light red color. These soils have a deficiency of humus, phosphorus, and nitrogen while minerals like lime and potash are in sufficient quantity. (ii) Stony and gravelly soils-Such soils contain large admixtures of gravels pebbles and cobbles and these are low-grade soil generally found at the base of the hills, and (iii) Lateritic soil. This soil appears brown or dark red in colour with high iron content due to lateralization of the weathered material in the favorable climate and topography. Suck kind of soil is found in the parts of Mandar, Bero, and Ratu blocks.

Rainfall

The average annual rainfall in the study area for the period 2001–2012 (12 years) was obtained from TRMM rainfall data (3B43). The TRMM product 3B43 provides gridded monthly rainfall data which was first converted into annual rainfall and the values were extracted at 18 selected locations in the study area. The average annual rainfall map of the study for the period 2001–2012 was created by interpolating the extracted rainfall data using spline interpolation routine in GIS environment.

Drainage density (D_d)

Dd is the spacing closeness of the stream channels with an inverse function of permeability (Agarwal and Garg 2016). It is also measured as the total length of the stream's channels per unit area. According to Prasad et al. (2008), a higher value of D_d infers to higher runoff capacity and less probability of groundwater recharge and vice-versa. Besides this, the drainage pattern also provides information about surface and sub-surface characteristics (Prasad et al. 2008).

The drainage density for the study area was obtained by integrating DEM and slope in a GIS environment. The drainage density of the study area was classified into five classes that included very high (1.5–2.5 km/km^2), high (1.0–1.5 km/km^2), moderate (0.6–1.0 km/km^2), low (0.3–0.6 km/km^2) and very low (0–0.3 km/km^2) class, respectively. Overall, the drainage density of the study area varied between 0 to 2.5 km/km^2.

Land use/land cover (LULC)

LULC influences the occurrence of groundwater (Murthy and Mamo 2009). The major LULC includes built-up area, agriculture, water bodies, forest, sandy area scrubland, and rocky areas. According to Mallick et al. (2014), agricultural regions are favourable for groundwater recharge. Conversely, the rocky areas have high runoff and less recharge capacity inferring to poor groundwater potential.

LULC map for the study area was prepared using Landsat 8 satellite data of May 2017. Supervised classification method using the maximum likelihood algorithm was applied to classify the satellite data because it is more widely used and reliable (Yinga et al. 2020). Additionally, on-screen visual interpretation techniques supported by the various interpretation keys including tone, texture, colour, shape, size, etc., were used in mapping various LULC classes in the study area. Toposheet and very high-resolution satellite data of Google Earth were used for ground-truthing.

Weight calculation

Weights were assigned to the various input data (geomorphology, lithology, LULC, drainage density, rainfall, soil, slope, and lineament density) that influence the presence of groundwater using AHP techniques. Paired wise comparison matrix was developed to compare all the parameters and their influence on groundwater by assigning specific values to these parameters. Saaty's (1980) method with a scale of 1–9 was adopted to determine the relative importance of all the aforementioned parameters.

Normalization of all the aforementioned parameters was done by assigning weights using Saaty's AHP in order to reduce the associated subjectivity. The normalization process converts the measurements of a set of objects on a standard scale into relative scale measurements (Saaty 1980). The nine-point scale of Saaty's method was used for assigning weights and setting criteria towards the analysis of groundwater prospect zones (Appendix 1). The consistency vector of the diagonal value of each criterion was calculated using the Eigenvalue matrix technique.

Following steps were employed for computing the final weights of all the parameters (Eq. 1, 2, 3, 4, 5, 6):

1. Sum of the values in each column of the pair-wise comparison matrix was computed as:

$$L_{ij} = \sum_{n=1}^{n} C_{ij} \tag{1}$$

where, L_{ij} is the total column value of the pair-wise comparison matrix and C_{ij} is the criteria used for analysis, i.e., drainage density, elevation, slope, etc.

2. Normalized pair-wise comparison matrix was computed as:

$$X_{ij} = \frac{C_{ij}}{\sum_{n=1}^{n} C_{ij}} \tag{2}$$

where X_{ij} = normalized pair-wise comparison matrix.

3. Standard weight was computed as:

$$X_{ij} = \frac{\sum_{j=1}^{n} X_{ij}}{N} \tag{3}$$

where W_{ij} = Standard weight and N = number of criteria/parameters.

4. Consistency vector values were computed as:

$$\lambda = \sum_{i=1}^{n} CV_{ij} \tag{4}$$

where λ = Consistency vector.

5. The consistency index (CI) used as a deviation or degree of consistency w computed as:

$$\mathrm{CI} = \frac{\lambda - n}{n - 1} \tag{5}$$

where CI = Consistency Index and n = Number of criteria.

6. Consistency ratio (Cr) was computed as:

$$\mathrm{Cr} = \frac{CI}{RI} \tag{6}$$

where RI = random inconsistency.

If the value of the Consistency ratio is less than or equal to 0.10, and then, the inconsistency is acceptable. Random inconsistency values for 'n' number of criteria, i.e., number of parameters are provided in Appendix 2.

Criteria weights assignment

All the input data/parameters (raster format) were assigned weights with respect to their respective role and influence on groundwater presence. The total score for each parameter was computed as (Saaty 1980) (Eq 7, 8):

$$\mathrm{TS} = \sum W \times R \tag{7}$$

where, TS = Total Score, W = weight of the parameters and R = weight of the features, respectively.

All the weighted parameters were integrated into a GIS environment and the groundwater potential zones were obtained as:

$$\mathrm{GWPZ} = \mathrm{L} + \mathrm{Ld} + \mathrm{G} + \mathrm{SL} + \mathrm{SO} + \mathrm{RF} + \mathrm{Dd} + \mathrm{LULC} \tag{8}$$

where, GWPZ = groundwater potential zone, L = lithology, G = geology/geomorphology, SL = slope, SO = soil, RF = rainfall, D_d = drainage density, and LULC = land use and land cover.

The percentage (%) of the area under groundwater was calculated using the equation given below (Eq. 9):

$$\text{Percentage of an area}\,(\%) = \frac{\text{estimated area}}{\text{total area}} * 100 \quad (9)$$

Sensitivity analysis

Each input parameter has its influence on the GWPZ, hence to better understand the overall influence, as well as the influence of the assigned rank and weights to each class and parameter, a sensitivity analysis was performed. The sensitivity analysis was performed using the following technique:

Map removal sensitivity analysis

The sensitivity of analysis was performed using the map-removal technique to determine the impacts of input parameters in the delineation of the GWPZ. Following this method, each input parameter/layer was removed sequentially from the GWPZ map and its impact with respect to remaining layers in the GWPZ map was expressed as (Eq. 10):

$$S = \left[(GWP/N) - \left(GWP'/n\right)/GWP\right] \times 100 \quad (10)$$

where S = index of sensitivity associated with the removal of a single parameter/layer, GWP is the groundwater potential index calculated using all parameters, GWP' is the groundwater potential index obtained by excluding each input parameter sequentially, N and n are the numbers of input parameters/layers used to calculate GWP and GWP′, respectively.

Evaluation of groundwater potential zone

The groundwater potential zone map was evaluated using well discharge data from fourteen dug wells obtained from the Central Ground Water Board, Ranchi, India. A correlation analysis was performed between groundwater potential map values obtained at the respective locations of dug wells and well discharge data.

Results and discussion

Weight assignment and normalization of thematic layers:

A pair-wise comparison of all the input parameters was computed in a square matrix, where diagonal elements of the matrix were always 1 (Table 1). The normalized pair-wise matrix was estimated using Eq. (2) and is presented in Table 2. The final normalized weights were obtained from Eq. (3) and are provided in Table 3.

Consistency analysis

The consistency vector was computed by multiplying pair-wise comparison matrix values with the normalized weights of the respective parameters/layers and was found to be 6.85. Further, consistency index (CI) and consistency ratio (CR) were calculated as -0.01 and -0.009, respectively. Since CR was less than 0.1, hence the inconsistency was found to be acceptable (Muralitharan and Palanivel 2015).

Rainfall

AHP method was used for assigning weight to the rainfall data layer. Pair-wise comparison and normalized weight were computed using the Eqs. 1–7. The consistency ratio for rainfall data was found to be -0.0046, suggesting a coherent matrix. The final weights for rainfall data layer were obtained by multiplying normalized weights of rainfall data layer (Table 2) to the normalized weight of individual features (Table 3). The final weights of the rainfall and its map for the study area are shown in Table 3 and Fig. 3, respectively.

Table 1 Pair-wise comparison matrix of seven thematic layers

Thematic layers	Lithology	Geomorphology	LULC	drainage density	Slope	Rainfall	Soil
Lithology	1	2	4	5	6	7	9
Geomorphology	0.5	1	2	4	5	6	7
LULC	0.25	0.5	1	2	4	5	6
Drainage Density	0.2	0.25	0.5	1	2	4	5
Slope	0.17	0.2	0.25	0.5	1	2	4
Rainfall	0.14	0.17	0.2	0.25	0.5	1	2
Soil	0.11	0.14	0.17	0.2	0.25	0.5	1
Total	2.37	4.26	8.12	12.95	18.75	25.5	34

Table 2 Normalized pair-wise matrix

Thematic layer	Lithology	Geomorphology	LULC	Drainage density	Slope	Rainfall	Soil	Total	Nor. Wt
Lithology	0.42	0.47	0.49	0.39	0.32	0.27	0.26	2.63	0.38
Geomorphology	0.21	0.23	0.25	0.31	0.27	0.24	0.21	1.71	0.24
LULC	0.11	0.12	0.12	0.15	0.21	0.19	0.18	1.09	0.16
Drainage Density	0.08	0.06	0.06	0.08	0.11	0.16	0.15	0.69	0.10
Slope	0.07	0.05	0.03	0.04	0.05	0.08	0.12	0.44	0.06
Rainfall	0.06	0.04	0.02	0.02	0.03	0.04	0.06	0.27	0.04
Soil	0.05	0.03	0.02	0.02	0.01	0.02	0.03	0.18	0.03

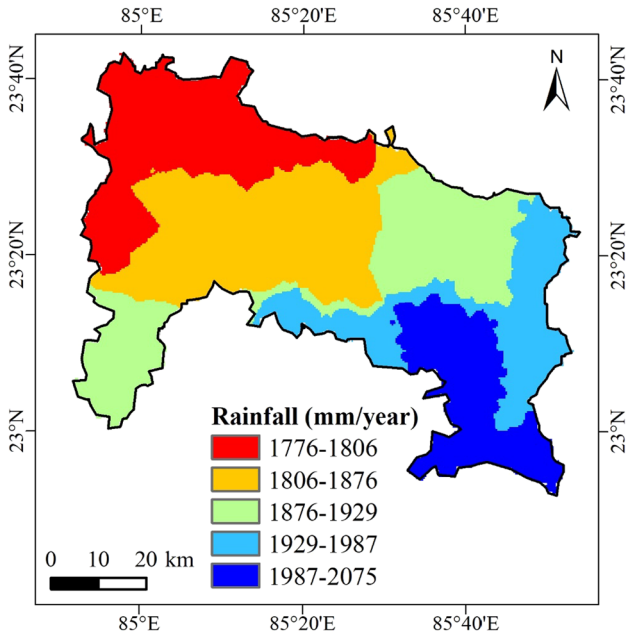

Fig. 3 Rainfall map

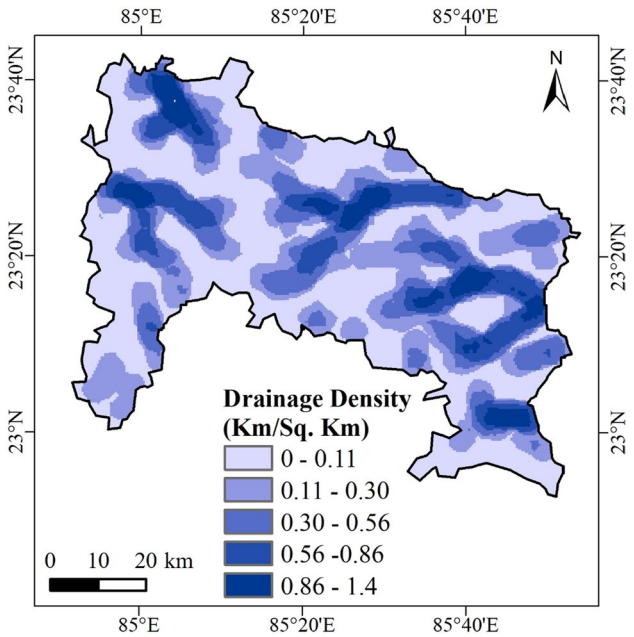

Fig. 4 Drainage density map

Drainage density (D_d)

AHP method was used to assign final weights to D_d data layer. Pair-wise comparison and normalized weight were computed using Eqs. 1–7. The CR for D_d data layer was found to be -0.008, which is less than 0.1, hence acceptable. The final weights of drainage density layers were obtained by multiplying normalized weights of D_d data layer with the normalized weight of individual features shown in Table 3. Figure 4 presents the drainage density map of the study area.

Land use/land cover (LULC)

The Consistency ratio for LULC data layer was found to be -0.0097, which is less than 0.1, hence the matrix is coherent. The final weight of LULC was obtained by multiplying normalized weights of LULC theme to the normalized weight of individual features presented in Table 3. The LULC map for the study area and its corresponding statistics are shown in Fig. 5 and Table 4, respectively.

Soil

Mainly three types of soil were found to be present in the study including sandy loam, silt loam, and sandy clay encompassing 36.11 (0.71%), 1863.43 (36.42%), and 3216.80 (62.87%) km^2, respectively. Ranks were assigned to the various soil types based on their respective infiltration rate. Clay loam soil was assigned the lowest rank due to a lesser infiltration rate, while sandy loam soil was assigned

Table 3 Normalized and final weights of different features of eight thematic layers for groundwater prospects

Sl. No	Theme	Normalized Weight (%)	Class	Final Weight
1	Lithology (LI)	38	River/Water Body	0.117
			Alluvium (Sand/Silt dominant)	0.083
			Sandstone, Shale, Coal	0.059
			Laterite	0.041
			Dolerite/Amphibolite (Basic Rocks),	0.029
			Quartzite	0.020
			Metamorphic Rocks	0.014
			Granite	0.010
			Mining areas	0.007
2	Geomorpholoy (GE)	24	River	0.011
			River sand	0.006
			Barakar formation	0.004
			Chotanagpur Granite Gneissic Complex	0.002
			Quartenary formation	0.001
			Pliestocene	0.001
3	Slope (%)	6	0–5	0.025
			5–15	0.016
			15–30	0.010
			30–40	0.006
			> 40	0.004
4	Soil	3	Sandy Loam	0.020
			Silt Loam	0.008
			Sandy Clay	0.003
5	Rainfall (RF) (mm/year)	4	1987–2075	0.018
			1929–1987	0.010
			1876–1929	0.006
			1806–1876	0.004
			1776–1806	0.002
6	Drainage Density (D_d) (km/km^2)	10	0–0.11	0.043
			0.11–0.30	0.026
			0.30–0.56	0.016
			0.56–0.86	0.010
			0.86–1.4	0.006
7	Land use/land cover (LULC)	16	Agriculture	0.069
			Forest	0.046
			Water body	0.025
			Forest	0.013
			Wasteland	0.007
			Built-up	0.069

the highest rank due to its higher infiltration rate and hence better groundwater potential.

The consistency ratio for soil data layer was found to be −0.0038 (i.e., > 0.1), resulting in a coherent matrix. The final weight of soil layers was obtained by multiplying normalized weights of soil data layers to the normalized weight of individual features. The soil map obtained for the study area is shown in Fig. 6.

Slope

The consistency ratio for the slope data layer was found to be -0.01, suggesting a coherent matrix. The slope map obtained was further reclassified into five classes that included very high (> 40%), high (20–40%), moderate (10–20%), low (4–10%), and very low (0–4%) class, respectively. Overall,

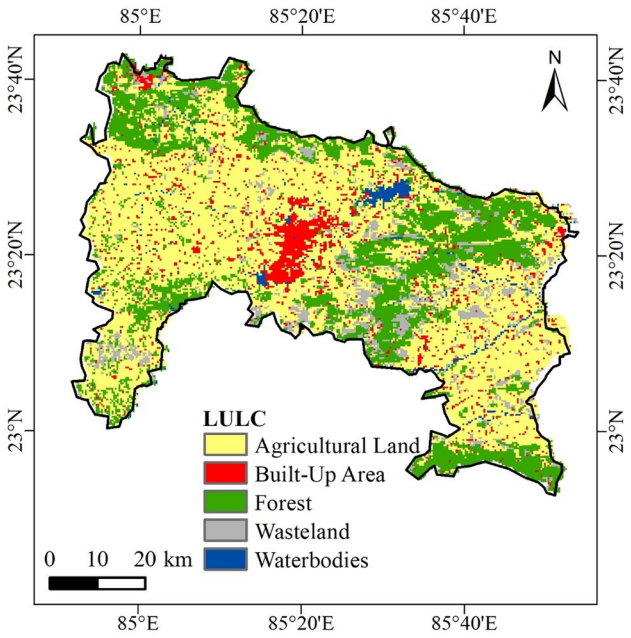

Fig. 5 LULC map

the slope in the study area varied between 0–121%. The slope map obtained for the study area is shown in Fig. 7.

Lithology

The study area is characterized by mainly eleven types of lithological units including river/water body, alluvium (sand/silt dominant), sandstone, shale, coal, laterite, dolerite/

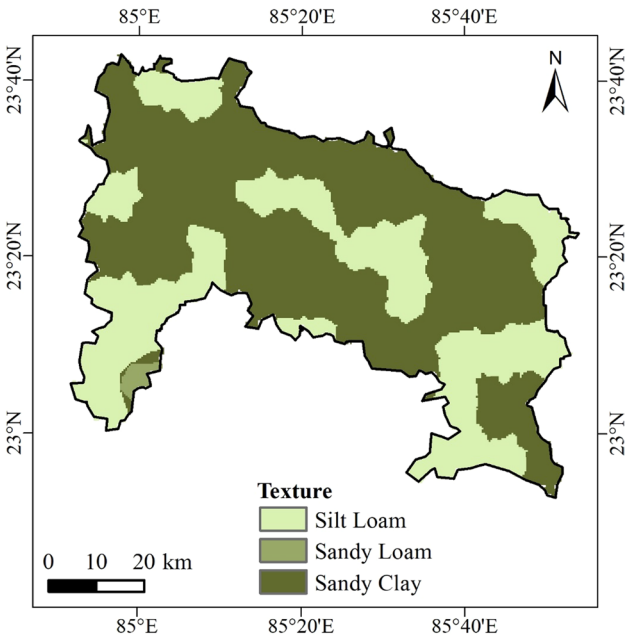

Fig. 6 Soil map

Table 4 Area statistics of land use land cover

Sl. no	Class name	Area statistics (km^2)	Percentage (%) of area
1	Agricultural Land	2889.754	56.46
2	Forest	1325.296	25.89
3	Waterbody	97.619	1.91
4	Wasteland	394.786	7.71
5	Built-up Area	410.77	8.03

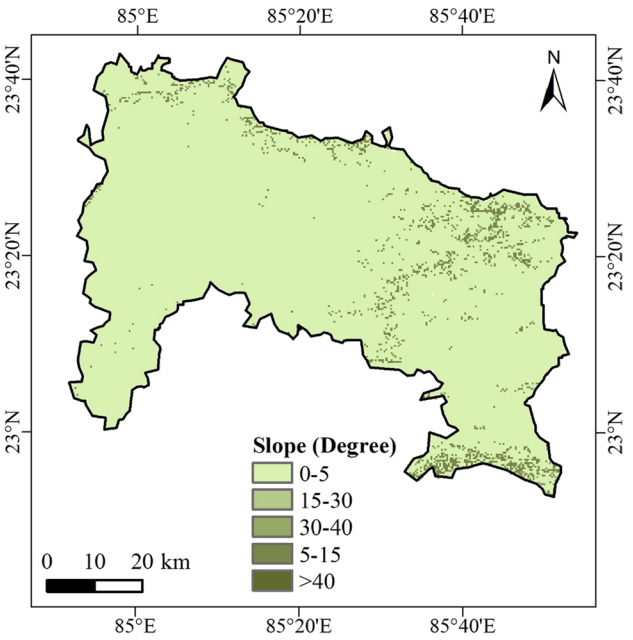

Fig. 7 Slope map

amphibolite (basic rocks), quartzite, metamorphic rocks, granite, and mining areas (Fig. 8). The largest lithologic unit in the study area is metamorphic rocks with an overall area of 4877.351768 km^2 (95.29%). The consistency ratio for the lithology data layer was found to be 0.058, suggesting a coherent matrix. The lithology map of the study area and its corresponding statistics are shown in Fig. 8 and Table 5, respectively.

Geomorphology

Study area consists of river sand, Barakar formation, Chota Nagpur granite gneissic complex, Quaternary formation, Pleistocene. Overall, the study area is dominated by Chota Nagpur granite-gneissic complex covering an area of 4914.35 km^2 (96.02%). The consistency ratio was found to be -0.0127 (i.e., < 0.1), suggesting a coherent matrix. The geomorphology map of the study area and its corresponding statistics are shown in Fig. 9 and Table 6, respectively.

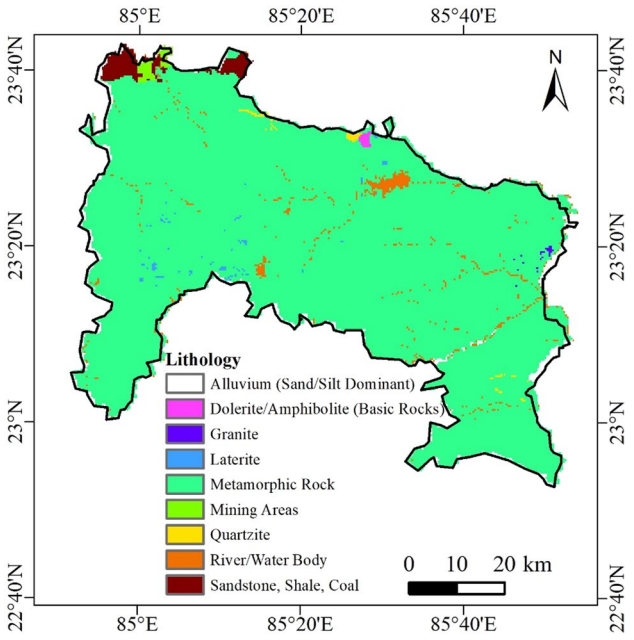

Fig. 8 Lithology map

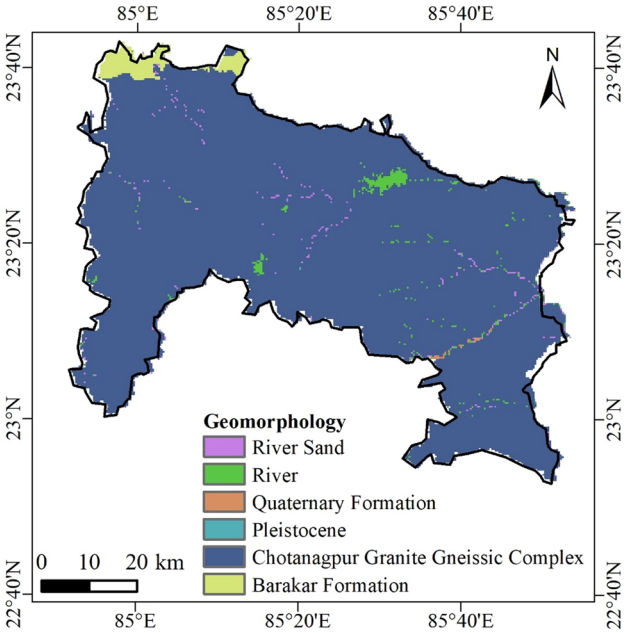

Fig. 9 Geomorphology map

Groundwater potential zones (GWPZ) Map

The GWPZ map of the study area was obtained by integrating all the normalized thematic layers in a GIS environment and converted into raster format. The GWPZ map was further processed by applying a majority filter to avoid/minimize pixel speckling. The GWPZ map was classified into four zones that included poor (8–9), moderate (9–10), good (10–13), and very good (13–24) potential zones, respectively. The GWPZ map obtained for the study area and corresponding statistics of the delineated zones are shown in Fig. 10 and Table 7, respectively.

Table 5 Area statistics of lithology

Feature	Area (km^2)	Percentage (%)
River/Water Body	101.51	1.98
Alluvium (sand/silt dominant)	4.63	0.09
Sandstone, shale, coal	75.98	1.48
Laterite	13.43	0.26
Dolerite/amphibolite (basic rocks)	6.48	0.13
Quartzite	13.76	0.27
Metamorphic Rocks	4877.35	95.29
Granite	4.72	0.09
Mining Areas	20.33	0.40

Validation of groundwater potential zones map

Individual zones delineated in the groundwater potential map were compared with the actual water level data (mean aquifer depth) for fourteen selected wells within the study area. A correlation analysis was conducted between the water level depth from the selected wells and scores from GWPZ obtained at the corresponding location of selected wells (Fig. 11 and Table 8)). The coefficient of determination (R^2) between the well data and GWPZ scores was found to be 0.59 indicating a plausible delineation of groundwater potential zones in the study area using remote sensing and GIS techniques along with AHP.

Sensitivity analysis

A sensitivity analysis was performed to determine the impact of the input data in delineating GWP zones. The results of

Table 6 Area statistics of geomorphology

Features	Area	Percentage (%)
River	64.27	1.26
River sand	38.29	0.75
Barakar formation	96.51	1.89
Chota Nagpur granite gneissic complex	4914.36	96.02
Quartenary formation	4.61	0.09
Pliestocene	0.078	0.00001

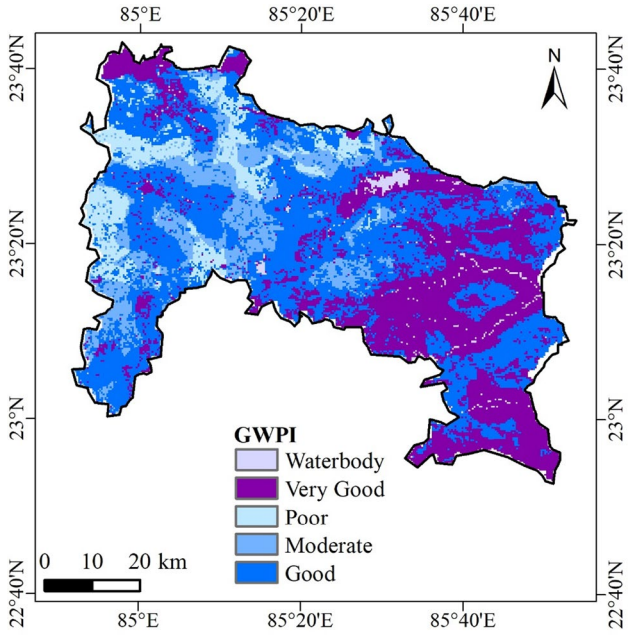

Fig. 10 Groundwater potential map

sensitivity analysis indicated that lithology and soil are the most and least sensitive parameters in delineating groundwater zones (Table 9).

Conclusions

The identification of groundwater recharge areas and delineation of potential zones are two important aspects for devising sustainable groundwater strategies. The groundwater occurrence depends on many biophysical indicators like rainfall, geology, geomorphology, hydrogeology, lineament density, lineament, drainage density, slope, soil, and presence of vegetation. In the present study, geomorphology, lithology, LULC, drainage density, rainfall, soil, slope, and lineament density were utilized for delineating GWPZ. The normalization of weights was calculated based on Saaty's AHP. All the aforementioned parameters were integrated into the GIS environment using weighted linear combination method

Table 7 Groundwater potential zones category and their distribution

Categories	Area (km^2)	Percentage (%)
Poor	411.79	8.53
Moderate	632.34	13.09
Good	2193.27	45.43
Very Good	1524.38	31.57
Water body	65.98	1.36

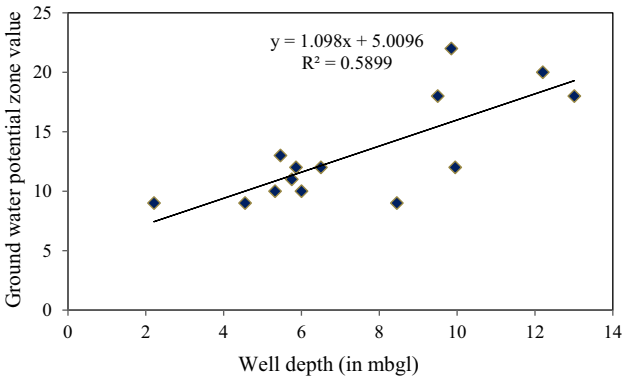

Fig. 11 Relationship between groundwater potential zone value and well depth point

and GWPZ were delineated for the study area. The delineated GWPZ map for the study area was obtained in a raster format and was classified into poor (8.53%), moderate (13.09%), good (45.43%), and very good (31.57%) zones, respectively. The left over area (1.36%) was found to be occupied by water bodies. The very good and good potential zones were found to be located in the east and central region of the study area, whereas most of the poor zones covered the west part.

The delineated GWPZ were evaluated through well discharge data using correlation analysis. The correlation analysis indicated that the integrated approach of remote sensing, GIS and AHP techniques followed for delineating GWPZ in the study area performed satisfactorily.

Future work can incorporate groundwater quality data also in delineating groundwater prospects.

Table 8 Selected wells with respective aquifer depths

Sl. No	Location	Water level (mbgl)
1	Buti	2.21
2	Ashoknagar	4.55
3	Jonha	5.46
4	Barwadag	5.75
5	Silli	5.86
6	Kathitanr	6
7	Ormanjhi	6.5
9	Mandar	8.45
9	Angara	9.85
10	Chachgura	9.95
11	Bero	13.01
12	Tamar	12.2
13	Bundu	9.5
14	Hatia	5.32

*mbgl (meters below ground level)

Table 9 Statistics of map removal sensitivity analysis

Layer removed	Statistical variation index (%)			
	Minimum	Maximum	Mean	Standard Deviation
L	0.74	3.2	2.8	4.21
L_d	0.04	0.39	1.78	1.69
G	0.42	0.44	0.55	1.70
SO	0.68	1.32	0.44	1.49
SL	1.34	1.02	1.9	2.80
RF	0.50	2.6	2.5	1.91
D_d	0.04	0.8	0.9	1.82
LULC	1.51	1.8	1.67	1.70

Appendix 1

Table 10.

Table 10 Scale for pair-wise comparison matrix

Intensity importance	1	2	3	4	5	6	7	8	9
Linguistic variables	Equal importance	Equal to moderate importance	Moderate importance	Moderate to the strong importance	Strong importance	Strong to the very strong importance	Very strong importance	Very to the extremely strong importance	Extreme importance

Appendix 2

Table 11.

Table 11 Random inconsistency values (Saaty 1980)

n	2	3	4	5	6	7	8	9
RI	0	0.52	0.9	1.12	1.24	1.32	1.41	1.45

Acknowledgment First author thanks to Lab of Centre for Geospatial Technologies, SHUATS, for providing the necessary facilities. The corresponding author express sincere thank to the DST-FIST, New Delhi, India for providing the infrastructural facilities to K. Banerjee Centre of Atmospheric and Ocean Studies, University of Allahabad, Prayagraj, India.

Funding The author received no specific funding for this work.

Declarations

Conflict of interest The authors declare they have no conflict of interests.

Ethical code of conduct We declare that we follow the journal guidelines.

References

Agarwal R, Garg PK (2016) Remote sensing and GIS based groundwater potential & recharge zones mapping using multi-criteria decision making technique. Water Resour Manag 30(1):243–260

Al-Abadi AM, Shahid S, Al-Ali AK (2016) A GIS-based integration of catastrophe theory and analytical hierarchy process for mapping flood susceptibility: a case study of Teeb area Southern Iraq. Environ Earth Sci. https://doi.org/10.1007/s12665-016-5523-7

Anbarasu S, Brindha K, Elango L (2020) Multi-influencing factor method for delineation of groundwater potential zones using remote sensing and GIS techniques in the western part of Perambalur district southern India. Earth Sci Inform 13(2):317–332. https://doi.org/10.1007/s12145-019-00426-8

Aouragh MH, Essahlaoui A, El Ouali A, El Hmaidi A, Kamel S (2017) Groundwater potential of Middle Atlas plateaus Morocco using fuzzy logic approach GIS and remote sensing. Geomatics, Nat. Hazards Risk 8(2):194–206. https://doi.org/10.1080/19475705.2016.1181676

Bellman RE, Zadeh LA (1970) Decision-making in a fuzzy environment. Manag Sci 17(4):B-141–B-164. https://doi.org/10.1287/mnsc.17.4.B141

Chen SJ, Hwang CL (1992) Fuzzy multiple attribute decision making methods. In Fuzzy multiple attribute decision making. Springer, Berlin, Heidelberg, pp 289–486

Chen W, Tsangaratos P, Ilia I, Duan Z, Chen X (2019) Groundwater spring potential mapping using population-based evolutionary algorithms and data mining methods. Sci Total Environ 684:31–49. https://doi.org/10.1016/j.scitotenv.2019.05.312

Central Groundwater Board (2013) Ground Water Information Booklet Ranchi District, Jharkhand State http://cgwb.gov.in/District_Profile/Jharkhand/RANCHI.pdf [Accessed date on: 29.09.2021]

Corsini A, Cervi F, Ronchetti F (2009) Weight of evidence and artificial neural networks for potential groundwater spring mapping: an application to the Mt. Modino area (Northern Apennines Italy). Geomorphology 111(1–2):79–87. https://doi.org/10.1016/j.geomorph.2008.03.015

Das S (2019) Comparison among influencing factor frequency ratio and analytical hierarchy process techniques for groundwater potential zonation in Vaitarna basin Maharashtra India. Groundw Sustain Dev 8:617–629. https://doi.org/10.1016/j.gsd.2019.03.003

Duan H, Deng Z, Deng F, Wang D (2016) Assessment of groundwater potential based on multicriteria decision making model and decision tree algorithms. Math Probl Eng 2016:1–11. https://doi.org/10.1155/2016/2064575

Duran-Llacer I, Arumí JL, Arriagada L, Aguayo M, Rojas O, González-Rodríguez L, Rodríguez-López L, Martínez-Retureta R, Oyarzún R, Singh SK (2022) A new method to map groundwater-dependent ecosystem zones in semi-arid environments: a case study in Chile. Sci Total Environ 816:151528. https://doi.org/10.1016/j.scitotenv.2021.151528

Kumar A, Pandey AC (2016) Geoinformatics based groundwater potential assessment in hard rock terrain of Ranchi urban environment, Jharkhand state (India) using MCDM–AHP techniques. Groundw Sustain Dev 2:27–41

Kumar N, Singh SK, Pandey HK (2018) Drainage morphometric analysis using open access earth observation datasets in a drought-affected part of Bundelkhand India. Appl Geomat 10(3):173–189. https://doi.org/10.1007/s12518-018-0218-2

Kumari A, Singh A (2021) Delineation of Groundwater Potential Zone using Analytical Hierarchy Process. J Geol Soc India 97(8):935–942

Lee S, Hong SM, Jung HS (2018) GIS-based groundwater potential mapping using artificial neural network and support vector machine models: the case of Boryeong city in Korea. Geocarto Int 33(8):847–861. https://doi.org/10.1080/10106049.2017.1303091

Lee S, Hyun Y, Lee S, Lee MJ (2020) Groundwater potential mapping using remote sensing and GIS-based machine learning technique. Remote Sens 12(7):1200. https://doi.org/10.3390/rs12071200

Machiwal D, Singh PK (2015) Comparing GIS-based multi-criteria decision-making and Boolean logic modelling approaches for delineating groundwater recharge zones. Arab J Geosci 8(12):10675–10691

Magesh NS, Chandrasekar N, Soundranayagam JP (2012) Delineation of groundwater potential zones in Theni district, Tamil Nadu, using remote sensing. GIS and MIF Techniques Geosci Front 3(2):189–196

Mukherjee S, Sashtri S, Gupta M, Sharma K (2007) Integrated water resource management using remote sensing and geophysical techniques: Aravali quartzite, Delhi, India. J Environ Hydrol 15:1–10

Muralitharan J, Palanivel K (2015) Groundwater targeting using remote sensing, geographical information system and analytical hierarchy process method in hard rock aquifer system, Karur district, Tamil Nadu. India Earth Sci Inform 8(4):827–842

Murmu P, Kumar M, Lal D, Sonker I, Singh SK (2019) Delineation of groundwater potential zones using geospatial techniques and analytical hierarchy process in Dumka district, Jharkhand. India. Groundw Sustain Dev 9:100239

Murthy KSR, Mamo AG (2009) Multi-criteria decision evaluation in groundwater zones identification in Moyale-Teltele sub-basin. South Ethiopia Int J Remote Sens 30(11):2729–2740

Nag SK, Kundu A (2018) Application of remote sensing, GIS and MCA techniques for delineating groundwater prospect zones in Kashipur block, Purulia district. West Bengal Appl Water Sci 8(1):1–13

Park S, Hamm SY, Jeon HT, Kim J (2017) Evaluation of logistic regression and multivariate adaptive regression spline models for groundwater potential mapping using R and GIS. Sustainability 9(7):1157. https://doi.org/10.3390/su9071157

Patle GT, Sikar TT, Rawat KS, Singh SK (2019) Estimation of infiltration rate from soil properties using regression model for cultivated land. Geol Ecol Landsc 3(1):1–13

Pande CB, Moharir KN, Panneerselvam B, Singh SK, Elbeltagi A, Pham QB, Varade AM, Rajesh J (2021) Delineation of groundwater potential zones for sustainable development and planning using analytical hierarchy process (AHP) and MIF techniques. Appl Water Sci. https://doi.org/10.1007/s13201-021-01522-1

Pandey HK, Singh VK, Singh SK (2022) Multi-criteria decision making and Dempster-Shafer model–based delineation of groundwater prospect zones from a semi-arid environment. Environ Sci Pollut Res. https://doi.org/10.1007/s11356-022-19211-0

Pourtaghi ZS, Pourghasemi HR (2014) GIS-based groundwater spring potential assessment and mapping in the Birjand Township southern Khorasan Province Iran. Evaluation de la potentialité des sources d'eau souterraine à partir d'un SIG et cartographie dans le district de Birjand Sud de la province de Khorasan Iran. Evaluación del potencial de manantiales de agua subterránea basado en GIS y mapeo en el Birjand Township sur de la provincia de Khorasan Irán. 伊朗Khorasan省南部Birjand镇基于GIS的地下水泉潜力评价和编图. Avaliação e mapeamento do potencial em nascentes de água subterrânea com base em SIG no município de Birjand sul da Província de Khorasan Irão. Hydrogeol J 22(3):643–662. https://doi.org/10.1007/s10040-013-1089-6

Prasad RK, Mondal NC, Banerjee P, Nandakumar MV, Singh VS (2008) Deciphering potential groundwater zone in hard rock through the application of GIS. Environ Geol 55(3):467–475

Rahmati O, Samani AN, Mahdavi M, Pourghasemi HR, Zeinivand H (2015) Groundwater potential mapping at Kurdistan region of Iran using analytic hierarchy process and GIS. Arab J Geosci 8(9):7059–7071

Rahmati O, Pourghasemi HR, Melesse AM (2016) Application of GIS-based data driven random forest and maximum entropy models for groundwater potential mapping: a case study at Mehran Region Iran. CATENA 137:360–372. https://doi.org/10.1016/j.catena.2015.10.010

Saaty TL (1980) The analytic hierarchy process, planning, priority setting, resource allocation. M cGraw-Hill, New York, p 287

Sikakwe GU (2020) Geospatial applications in delineating groundwater prospect zones in a hard rock terrain: an integrated approach. Environ Earth Sci 79(21):1–18

Singh S, Singh C, Mukherjee S (2010) Impact of land-use and land-cover change on groundwater quality in the Lower Shiwalik hills: a remote sensing and GIS based approach. Open Geosci 2(2):124–131

Singh S, Singh C, Kumar K, Gupta R, Mukherjee S (2009) Spatial-temporal monitoring of groundwater using multivariate statistical techniques in Bareilly district of Uttar Pradesh, India. J Hydrol Hydromech 57(1):45–54

Trabelsi F, Lee S, Khlifi S, Arfaoui A (2018) Frequency ratio model for mapping groundwater potential zones using GIS and remote sensing; Medjerda Watershed Tunisia. In Conference of the Arabian Journal of Geosciences. Springer, Cham, pp 341–345

Singh VK, Kumar D, Kashyap PS, Singh PK, Kumar A, Singh SK (2020) Modelling of soil permeability using different data driven algorithms based on physical properties of soil. J Hydrol 580:124223

Yinga OE, Kumar KS, Chowlani M, Tripathi SK, Khanduri VP, Singh SK (2020) Influence of land-use pattern on soil quality in a steeply sloped tropical mountainous region India. Arch Agron Soil Sci. https://doi.org/10.1080/03650340.2020.1858478